# 1

# Introduction to High-Entropy Materials

The advancements of human civilization are largely determined by the materials and tools that were manufactured and mastered by humans. During the Stone Age, the ancient human could use only natural materials, including stone, bone, and wood. After that, with the capability of reduction and extraction of copper, tin, lead, and iron from their ores, tools made of copper and iron were widely used in daily life, transportation, and construction during the Bronze Age and the Iron Age. Nowadays, more and more materials with specific properties and performance have been discovered and utilized due to the more efficient metallurgy techniques and material design paradigms, as shown in Figure 1.1 [2]. In the early stage of material design, one principal element is chosen and alloyed with other elements in trace amount to improve the properties of the original element. This design strategy is still dominant in our material design, such as Al alloys, Ni alloys, Fe alloys, and binary solid solution ceramics. Thus, information and understanding are highly developed on materials close to the corners and edges of a multicomponent phase diagram, with little known about those located at the center of the diagram [1, 3]. Recently, crystalline multi-principal element materials located at or near the center of the phase diagram with equal or near-equal atomic fraction of constituting elements have been introduced and have attracted increasing attention due to their unique compositions, microstructure, and unexpected properties. In this chapter, the basic concepts and information about these fascinating materials will be reviewed.



## 1.1 History of High-Entropy Materials

Attempts to synthesize multicomponent alloys were driven by the desire of metallic glasses with super-high glass-forming ability. After examining the works of Inoue et al. and Peker et al. [4, 5], Greer proposed a "confusion principle," which states that the more the number of elements involved, the lower is the chance that the alloy could

*High-Entropy Materials: From Basics to Applications,* First Edition.
Huimin Xiang, Fu-Zhi Dai, and Yanchun Zhou.

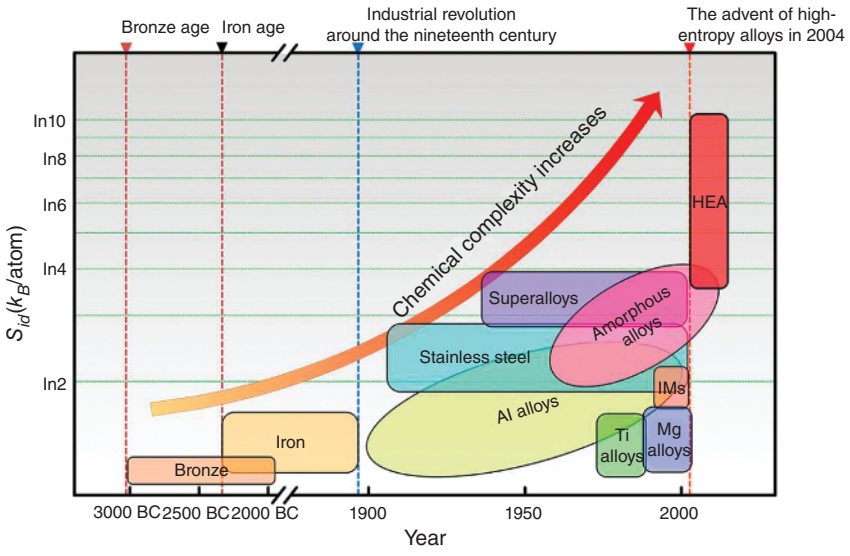


**Figure 1.1** Rising trend of alloy chemical complexity versus time (IMs: intermetallics or metallic compounds, HEA: high-entropy alloy). Source: Reproduced with permission from Cantor [1]/Springer Nature.

select viable crystal structures, and the greater is the chance of glass formation [6]. He also pointed out that the most "confused" elements were those that differed most from each other in size. This principle has boosted the subsequent search of metallic glasses in multicomponent alloys with large atomic size difference [7–9].

In 2004, two independent papers regarding multicomponent alloys have been published by Yeh et al. and Cantor et al. [10, 11]. Their results seemed to falsely verify the principle of confusion. In Cantor's paper, entitled "Microstructural development in equiatomic multicomponent alloys," the authors performed induction melting and melt quenching rapid solidification experiments on an equiatomic mixture of 20 elements (Mn, Cr, Fe, Co, Ni, Cu, Ag, W, Mo, Nb, Al, Cd, Sn, Pb, Bi, Zn, Ge, Si, Sb, and Mg) and 16 elements (Mn, Cr, Fe, Co, Ni, Cu, Ag, W, Mo, Nb, Al, Cd, Sn, Pb, Zn, and Mg) [11]. Surprisingly, instead of glassy phases, these alloys were multiphase, crystalline, and brittle, even after melt spinning. Moreover, they found that these alloys consisted predominantly of a single face-centered cubic (FCC) primary phase containing many elements but particularly rich in transition metals, notably Cr, Mn, Fe, Co, and Ni. Based on these results, they designed and prepared an equimolar $Cr_{20}Mn_{20}Fe_{20}Co_{20}Ni_{20}$ alloy with a single FCC structure and a typical dendritic microstructure in the as-cast condition. They also found that the total number of phases was always well below the maximum equilibrium number allowed by the Gibbs phase rule and even further below the maximum number allowed under non-equilibrium solidification conditions. They argued that the confusion principle might not apply and other factors were more important in promoting glass formation rather than chemical complexity.

Simultaneously, Yeh et al. published the paper entitled "Nanostructured high-entropy alloys with multiple principal elements: novel alloy design concepts and outcomes," and clearly defined the term of high-entropy alloys (HEAs) [10]. By rough estimation of mixing entropies of multiple-principal-element alloys, they found that the mixing entropy of alloys with five or more constituent elements was larger than that of metal fusion and formation enthalpies of strong intermetallic (IM) compounds, indicating the preferred tendency of formation of random solid solutions during solidification of these alloys. Due to the central role of mixing entropy in stabilizing the solid solution, they defined these alloys as HEAs. They took the as-cast $CuCoNiCrAl_xFe$ alloy system as an example to illustrate that how simple the structure of these chemically complex alloys could be. In the same paper, they also concluded some conspicuous properties of HEAs, such as nanostructures resulting from difficulty in substitutional diffusion of elements, high hardness induced by multi-strengthening mechanisms, excellent resistance to annealing softening, wear, and oxidation. These promising properties made HEAs potentially suitable for many applications such as tools, molds, dies, mechanical parts as well as anticorrosive high-strength parts in chemical plants, integrated circuit (IC) foundries, and even marine applications. Moreover, unlike the commonly used traditional alloy systems, the number of HEAs was countless, even after excluding chemically incompatible elements that produced liquid immiscibility, and the concept of HEAs led to a whole new and uncharted territory, in which many possible new materials, phenomena, theories, and applications were awaited [9].

These two innovative works have ignited enthusiastic research on HEAs. It is worth mentioning that, before they published their groundbreaking works, years of related and ground works have been conducted. Cantor started the study of multicomponent alloys consisting of a large number of constituents in equal or near-equal proportions with his undergraduate students since the beginning of 1980s [12], while the exploration on multicomponent alloys by Yeh and his students could be traced back to 1995 [13].

The attempts to search high-entropy ceramics (HECs) were started by Chen et al. in their pursuit of promoting the hardness of HEA films by introducing non-metallic elements, such as nitrogen and oxygen [14–16]. They found that introducing nitrogen into $Al_{0.5}CoCrCuFeNi$, $Al_2CoCrCuFeNi$, and AlCrNiSiTi resulted in the amorphization and hardening of the nanostructured metallic solid solution [14, 15]. The oxidation of $Al_xCoCrCuFeNi$ ($x = 0.5, 1, 2$) HEAs led to the formation of a single cubic-spinel crystalline phase [16]. Although they synthesized the ceramics with multi-principal elements, the concept of high-entropy-stabilized ceramics was not used to describe these materials until Rost et al. published their work on high-entropy oxides (HEOs) with a single rock-salt phase and five different cations in equiatomic fractions [17]. This work has led to a significant increase in the number of publications about HEOs, and up to now, a large part of the publications is related to HEOs due to their fascinating mechanical and functional properties. Inspired by this work, high-entropy borides, high-entropy carbides, and other non-oxide HECs have been discovered and reported subsequently [18–21].

## 1.2 Definition of High-Entropy Materials

There are two generally accepted and widely used definitions for HEAs. One is based on composition and the other is based on configurational entropy. The first one was proposed in 2004 by Yeh et al. based on the compositional requirements [10]. They defined the HEAs as those containing at least five major principal elements with the concentration of each element being between 35 and 5 at.%. In their definition, the ratio of the major elements was not restricted to be equimolar, taking $CuCo_{0.5}Ni_{1.2}CrAlFe_{1.5}Ag_{0.02}B_{0.1}C_{0.15}$ as an example, leading to countless high entropy (HE) alloys with multiple principal elements. Moreover, HEAs were not required to be a single-phase solid solution according to this definition, and $CuCoNiCrAl_xFe$ alloys with $0.8 < x < 2.8$ was an illustration.

The second definition is based on the magnitude of mixing entropy. According to the Boltzmann's thermodynamic statistics principle, the quantitative relationship between the entropy and complexion of the system is given by:

$$\Delta S_{conf} = k \ln \omega \tag{1.1}$$

where $k$ is the Boltzmann's constant, and $\omega$ is the thermodynamic probability, which represents the total number of microscopic states contained in the macroscopic state. With the increase in the number of microscopic states, the configuration entropy of the system increases. For a solid solution consisting of $n$ kinds of atoms, the configurational entropy can be estimated by:

$$\Delta S_{conf} = -R\left[c_1 \ln c_1 + c_2 \ln c_2 + \cdots + c_n \ln c_n\right] = -R\sum_{i=1}^{n} c_i \ln c_i \tag{1.2}$$

where $R$ is the gas constant, $c_i$ is the mole fraction of the $i$th element, and $n$ is the total number of components. According the extreme value theorem, the configurational entropy reaches its maximum value when the mole fraction of all elements is equal, which is $R\ln n$. Yeh calculated the configuration entropies of equimolar alloys with constituent elements up to 13 [22]. Comparing the configurational entropy of a three-element equimolar alloy and a five-element alloy, they believed that $1.5R$ was large enough to compete with mixing enthalpy as well as to be used as a border line between HEAs and medium-entropy alloys (MEAs). In addition, $1R$ was used to separate the MEAs and low-entropy alloys (LEAs). Accordingly, the alloy world could be categorized, as shown in Figure 1.2. They also suggested a practical upper bound of 13 principal elements for HEAs, since the benefit from the high-entropy effect of more principal elements was quite limited with the cost of complexity in handling raw materials or recycling the alloys.

Generally, the HEAs defined by these two definitions overlap with each other in most cases. Still, some exceptions exist. For $FeCoNiAl_{0.2}Si_{0.2}$ alloy [23], it can be recognized as HEA by the composition definition since it contains five principal elements with the atomic percentage larger than 5 at.%. However, the configurational entropy of this alloy is approximately $1.41R$, which is located in the MEA

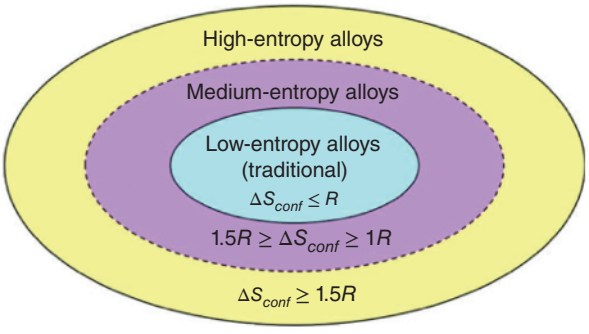


**Figure 1.2** Alloy world based on configurational entropy. Source: Reproduced with permission from Yeh [22]/Springer Nature.

territory according to the entropy definition. On the other hand, with the development of novel synthesis method, the number of constituent elements that could mixed in one alloy progressively increases. Extreme mixing of 15 and 21 metals in one alloy has been recently reported [24, 25]. For the alloy containing 21 elements, the concentration of each element is smaller than 5 at.%, which cannot fit the composition definition but still can be regarded as HEA due to its large mixing entropy. As stated by Yeh, it is not easy to give a clear-cut definition for HEAs, and these two definitions are just guidelines for the design of HEAs [22].

The concept and definition of HECs are inherited from those of HEAs. Due to the existence of more than one sublattice in the structure, the molar configurational entropy of HECs should be calculated by [26]:

$$\Delta S_{conf} = -R\sum_{j=1}^{n}\sum_{i=1}^{m} c_i^j \ln c_i^j \tag{1.3}$$

where $c_i^j$ represents the mole fraction of elements in the $j$th sublattice. Similarly, with the mixing entropy larger than 1.5$R$, the ceramic solid solution can be classified as HECs. From Eq. (1.3), it is quite clear that for ceramics with chemical disorder in more than one sublattice, the mixing entropy is significantly larger than that of HEAs. We should emphasize that, for both HEAs and HECs, the composition and entropy definitions are just guidelines without the guarantee of formation of a single-phase solid solution.

## 1.3 Core Effects of HEMs

Based on their ground research studies, Yeh summarized mainly four core effects for HEAs, which were as follows: (i) thermodynamics: high-entropy effects, (ii) structure: lattice distortion, (iii) kinetics: sluggish diffusion, and (iv) properties: cocktail effects [22, 27].

### 1.3.1 High-Entropy Effect

The high-entropy effect is the most important for HEAs since it promotes the formation of random solid solution alloys with a simple structure rather than intermetallic compounds in multicomponent alloys. Thermodynamically, the state having the lowest mixing free energy $\Delta G_{mix}$ among all possible states would be the equilibrium state. The mixing free energy is determined by the competitive mixing enthalpy $\Delta H_{mix}$ and entropy $\Delta S_{mix}$ by: $\Delta G_{mix} = \Delta H_{mix} - T\Delta S_{mix}$. For a solid solution with a large number of elements, the mixing entropy is high, as discussed in Section 1.2, and it becomes more dominant at higher temperatures. Therefore, the significantly higher mixing entropy of HEAs for the random solution state is expected to significantly extend the solubility range for terminal solutions and form simple multielement solution phases, especially at higher temperatures. The formation of single-phase CrMnFeCoNi alloy is a vivid illustration of competition of enthalpy and entropy. For this alloy system, the as-cast ingot exhibited a typical dendrite structure from its melts with a single FCC structure [11], indicating the random occupation of all elements in a solid solution. However, minor precipitates on the grain boundaries of samples annealed at temperatures lower than 800 °C were found and determined to be intermetallics [28, 29]. The metastable nature of CrMnFeCoNi HEA demonstrated the significant role of mixing entropy in the formation of this single phase at high temperature. This effect has also been used to understand the formation of single phase HEOs, (CoCuMgNiZn)O [17]. Rost et al. found an endothermic reaction upon cyclic heat treatment of rocksalt (CoCuMgNiZn) O HEO. They attributed this to the enthalpic penalties of Zn and Cu for crystallization of a rocksalt structure. To lower the barrier of formation of a single solid solution, these two elements were excluded from HEO. However, this was not the case, exclusion of Zn and/or Cu led to the formation of multiphases. This was a strong indication that the role of mixing entropy was prominent, since it decreased when one cation was removed.

Although high-entropy effect is important for the formation of HEMs, it is not the only factor that determines the phase formation for multicomponent alloys and ceramics, as will be discussed in Chapter 2.4. Nevertheless, it is still the core effect for HEM formation and reduces the number of phases as predicted by Gibbs phase rule that permits the number of phases in equilibrium to increase with the number of components.

### 1.3.2 Lattice Distortion

This structure feature is quite obvious due to the random distribution of different atoms with different atomic size in one structure, as schematically illustrated in Figure 1.3 [30]. Also, due to the different electronegativity of atoms, the bonding strength and bond length between atoms differ from each other, which is also responsible for the lattice distortion. This crystal feature was proposed by Yeh et al. in the investigation of CuCoNiCrAlFeTiV alloys [31], and the effects on the X-ray diffraction (XRD) intensities of CuNiAlCoCrFeSi alloy were mathematically

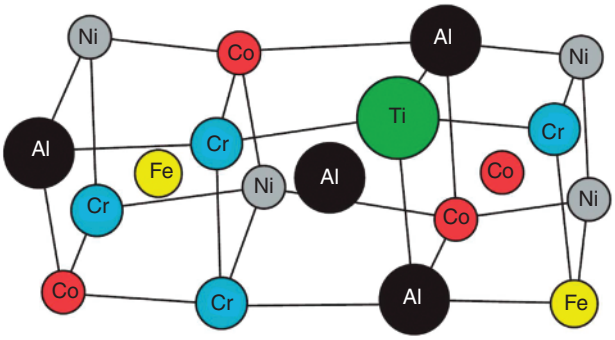


**Figure 1.3** A schematic illustration of serious distorted $AlCoCrFeNiTi_{0.5}$ lattice.
Source: Reproduced with permission from Zhang et al. [30]/John Wiley & Sons.

determined [32]. With the help of various characterization techniques, lattice distortion was observed in multiple HEAs and ceramics [33–37].

In addition to the reduction in the intensity of XRD pattern, lattice distortion is also used to explain the variation in other properties. Lattice distortion can hinder dislocation motion and result in significant solid solution strengthening effects [10]. It is also responsible for the severe scattering of electrons and phonons, leading to the significant decrease in electric and thermal conductivity and weak temperature dependency of the transport properties [38]. It might also lead to the amorphization when sufficiently large atomic size differences collapse the distorted lattice. The influence of lattice distortion on the properties of HEMs will be discussed in Chapter 7.

### 1.3.3 Sluggish Diffusion

Atom diffusion in the matrix is an important process in the formation of new phases and grain growth, and it is closely related to the high-temperature strength and structure stability. This effect has been used to explain the formation of nano-precipitates in the as-cast HEA matrix [10], and easier formation of amorphous structure for a higher number of elements in HEAs [27].

To verify this effect, Tsai et al. examined the diffusion phenomenon of constituent elements in a quinary HEA, $CoCrFeMn_{0.5}Ni$ [39]. Through theoretical analysis, they were able to determine the intrinsic diffusion coefficients from quasi-binary diffusion couples and validate the comparison of their data with other tracer-based diffusion results. The measured diffusion rate of elements in $CoCrFeMn_{0.5}Ni$ decreased in the sequence of Mn, Cr, Fe, Co, and Ni. The extrapolation values of the diffusion coefficients for each element at the melting point, $D_{T_m}$, were the smallest in the Co–Cr–Fe–Mn–Ni alloy system, comparing with other FCC matrices, including Fe–Cr–Ni–(Si) alloys, Fe, Co, and Ni. In addition, the activation energies normalized by melting points, $Q/T_m$, of all elements in HEA were the largest. They concluded that these results were direct evidence for the sluggish diffusion effect in HEA. The origin of the sluggish diffusion effect was also identified to be the fluctuation in lattice

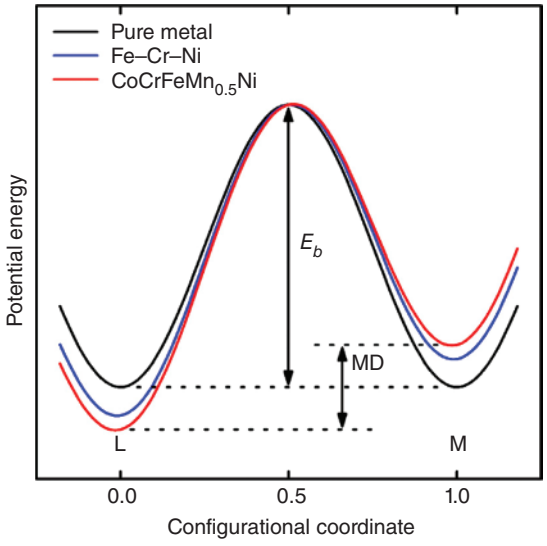


**Figure 1.4** Schematic diagram of the variation in lattice potential energy (LPE) and mean difference (MD) during the migration of a Ni atom in different matrices. The MD for pure metals is zero, whereas that for HEA is the largest. Source: Reproduced from Tsai et al. [39]/ with permission of Elsevier.

potential energy (LPE) by calculating the so-called seven-bond interaction energy (SBIE, which represents the energy difference before and after the atomic migration) using a pair potential or quasi-chemical model. They found that the mean difference (MD) values of SBIE in different matrices were quite different. The calculated MD for Ni in HEA was nearly 1.5 times of those in Fe–Cr–Ni ternary alloys, indicating that a diffusing Ni atom experienced significantly greater LPE fluctuation in HEA than in traditional alloys. As illustrated in Figure 1.4, due to the existence of MD in LPE of HEAs and traditional alloys, the transition frequencies between adjacent lattice sites were asymmetric, and the atoms preferred to stay at lattice sites with lower LPE, which served as atomic traps that hinder diffusion. The larger the LPE fluctuation, the stronger is the trapping effect, and the lower the diffusion rate would be.

On the other hand, Miracle et al. argued that the measured diffusion coefficients in $CoCrFeMn_{0.5}Ni$ were not essentially different from diffusion in elements and conventional alloys [40]. The data they extracted from the experiments demonstrated that diffusion coefficients in $CoCrFeMn_{0.5}Ni$ were generally higher than in conventional materials when compared at the same temperature, as shown in Figure 1.5. For instance, at 1173 K, the diffusion coefficients of Ni in $CoCrFeMn_{0.5}Ni$, Fe–15Cr–20Ni, and pure Fe were $14.3\times10^{-18}$ $m^2/s$, $6.56\times10^{-18}$ $m^2/s$, and $3.12\times10^{-18}$ $m^2/s$, respectively. Moreover, the higher activation energies normalized by melting points was based on the empirical observation that diffusion coefficients at $T_m$, $D_{T_m}$, were roughly equal for alloys with similar crystal structure and bonding type, and the value of $D_{T_m}$ for all elements in HEA fell in the range of $D_{T_m}$ values in pure metals and binary alloys, thus demonstrating no significant difference between HEA and conventional alloys in diffusion when the data were normalized at $T_m$.

Controversy exists on this structure characteristic, and additional works on the intrinsic diffusion coefficients in HEAs may be needed, which is challenging

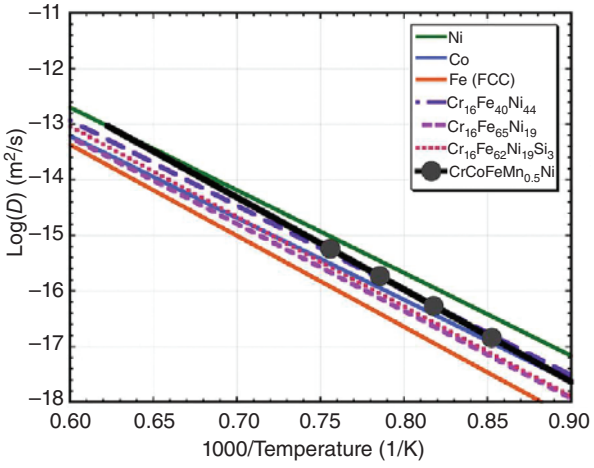


**Figure 1.5** Diffusion coefficients of Ni in FCC elements, stainless steel alloys (compositions in the legend are shown in at.%) and $CoCrFeMn_{0.5}Ni$ as a function of inverse absolute temperature. Source: Reproduced from Miracle et al. [40]/with permission of Elsevier.

in experiment. Nevertheless, more atomic diffusion relation phenomena have been reported, such as good irradiation resistance and slow grain growth [41, 42].

### 1.3.4 Cocktail Effect

The initial intent of Ranganathan using the phrase of "multimetallic cocktails" was to emphasize alloy pleasures in alloy design and development [43]. In HEMs, cocktail effect is used to emphasize a synergistic effect of the whole properties from the overall contribution of the constituent elements. Considering the expanded solubility of different elements in HEMs, the design freedom of HEMs is huge, which gives great opportunity for property adjustment in HEMs based on the mixture rule since different elements with different chemical states and properties can be selected. Moreover, because of the mutual interactions among the elements, unexpected results could be obtained through synergistic effect.

The central idea of cocktail effect is that the properties of HEMs are designable by adding proper ingredient according to the mixture rule. For example, the hardness of body-centered cubic (BCC) structured material is normally higher than that of FCC structured material due to the limited slip systems. Thus, by adjusting the content of BCC phases, the hardness of HEAs changes accordingly. Al element is a strong BCC stabilizer, and adjusting the content of Al can control the content of BCC phases. As demonstrated by Yeh et al., with the Al content increasing in $CuCoNiCrAl_xFe$ HEA, the phases changed from FCC to BCC + FCC and finally to BCC structure [10]. The lattice constant for both the FCC and BCC structures increased as well as the hardness of the HEA. This situation was also observed in Cu-free $Al_xCoCrFeNi$ HEA [44]. Another example on the application of cocktail effect is the property optimization of a soft magnetic HEA, $FeCoNi(AlSi)_x$ alloys [45].

For an applicable soft magnetic material, high saturation magnetization, electrical resistivity, and malleability are required. Due to their ferromagnetic nature, Ni, Co, and Fe elements are positive to the improvement of saturation magnetization. However, experimentally proved low electrical resistivity of NiCoFe MEAs brought large eddy current loss. To optimize the combinational properties of NiCoFe MEA, Al and Si were chosen. First, the nonmetal element Si was known to increase the electrical resistivity, while large Al atoms led to severe lattice distortion that could scatter the electrons efficiently. Secondly, co-doping of smaller Si and larger Al atoms enhanced the crystal lattice distortion, resulting in a solid solution-strengthening effect that could promote the mechanical property. Thus, mixing of Ni, Co, Fe, Al, and Si could lead to a satisfactory result. By careful adjustment of Al and Si content, Zhang et al. found that the alloy with the composition of $FeCoNi(AlSi)_{0.2}$ had the best combination of $M_s$ (1.5 T), $H_c$ (1400 A/m), $\rho$ (69.5 μΩ·cm), and $\varepsilon_p$ (>50%) for application as a soft magnetic material [45].

Some deviations from the mixture rule are often observed in HEMs due to the synergistic effect. In the hardness measurements of high-entropy borides, Gild et al. found that the measured hardness of six single-phase high-entropy metal diborides were generally greater than the averages of the hardness values measured from individual metal diborides [18], as shown in Figure 1.6. In addition, thermal expansions that depart from their average values have also been reported in HEAs and HECs, which will be discussed in Chapter 7 [46–48].

Due to the existence of cocktail effect, designing HEMs with desired properties is feasible. It is important for one to comprehensively consider various factors involved before selecting appropriate composition and processes. Moreover, one has to keep in mind that unexpected result that can come from the unusual synergistic interactions between the selected elements.

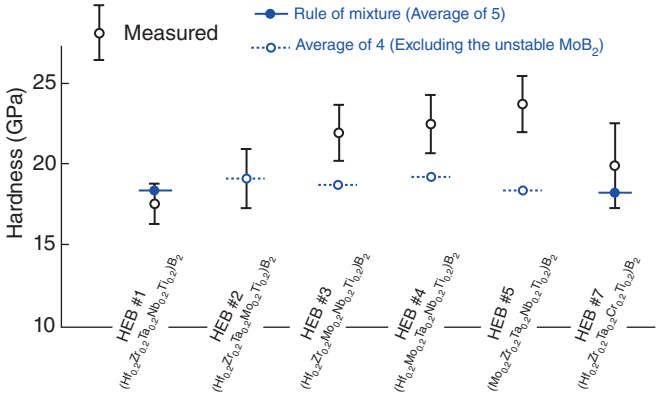


**Figure 1.6** Measured hardness of high-entropy borides and the average values from the rule of mixture of individual metal diborides. Source: Gild et al. [18]/Springer Nature/ CC BY-4.0.

## 1.4 Development of the HEMs

In the early stage of HEAs investigations, most of the works aimed to achieve a single phase with superior properties from equal or near-equal atomic fraction of constituting elements. With the development of HEAs, it is found that HEAs with non-equimolar compositions or multiphase structure prevail in mechanical properties. For instance, Li et al. developed a new class of transformation-induced plasticity-assisted dual-phase (TRIP-DP) $Fe_{50}Mn_{30}Co_{10}Cr_{10}$ HEA, which overcame the strength–ductility trade-off, as shown in Figure 1.7 [49]. By departing from equiatomic composition, the stability of this HEA decreased with two key benefits: interface hardening due to a dual-phase microstructure and transformation-induced hardening, leading to the simultaneous increase in strength and ductility. Lu et al. proposed a novel strategy to design HEAs using the eutectic alloy concept to solve the strength–ductility paradox, inferior castability, and segregation issues of HEAs [50]. The eutectic-like microstructure that consisted of an alternate layer of soft FCC and brittle BCC phases was developed in $AlCrFeCoNi_{2.1}$ HEA. This alloy exhibited unusual work hardening behavior, attributing to the fine lamellar structure. They also proposed a strategy, specifically, through calculation of mixing enthalpy, to locate eutectic compositions in HEAs [51], and designed a series of eutectic HEAs containing Zr, Hf, Nb, and Ta. The complete eutectic

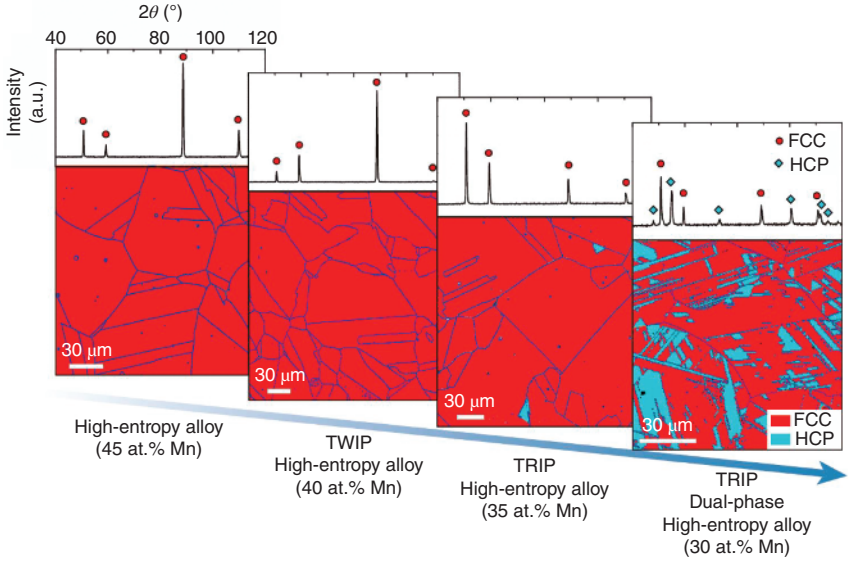


**Figure 1.7** XRD patterns and electron backscatter diffraction (EBSD) phase maps of $Fe_{80-x}Mn_xCo_{10}Cr_{10}$ ($x$ = 45 at.%, 40 at.%, 35 at.%, and 30 at.%) HEAs. The Mn content plays an important part in phase constitution and tuning phase stability for the activation of specific displacing transformation mechanisms. Source: Reproduced with permission from Li et al. [49]/Springer Nature.

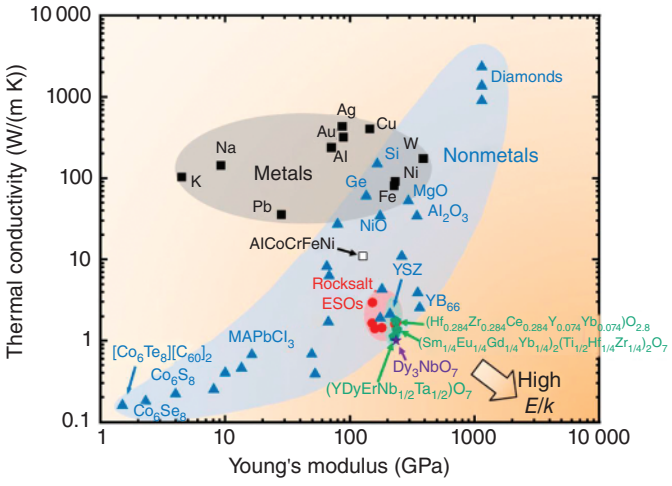


**Figure 1.8** Thermal conductivity ($\kappa$) versus Young's modulus ($E$) of several types of materials to feature several HECs/CCCs with a high $E/\kappa$ ratio. ESO = entropy-stabilized oxide. Source: Reproduced with permission from Wright et al. [55]/Springer Nature.

structures were observed in $Zr_{0.6}CoCrFeNi_{2.0}$, $Nb_{0.74}CoCrFeNi_{2.0}$, $Hf_{0.55}CoCrFeNi_{2.0}$, and $Ta_{0.65}CoCrFeNi_{2.0}$ HEAs. These results demonstrate impressive comprehensive performance of HEAs with non-equimolar compositions or multiphase structure, which is considered as the next-generation HEAs [52].

Inspired by the exciting discovery in the field of HEAs, Wright et al. proposed to expand HECs to compositionally complex ceramics (CCCs) to include non-equimolar compositions [53]. They found in their works that the ideal mixing (configurational) entropy was not the best descriptor to describe thermal conductivity and high configurational entropy could not guarantee low thermal conductivity [53, 54]. For instance, the nominal oxygen vacancy concentration determined the thermal conductivity of Yttria-stabilized zirconia (YSZ)-like fluorite oxides, while in cubic pyrochlore oxides, size disorder governed the thermal conductivity. These combined studies demonstrated that various medium-entropy compositions could outperform their high-entropy counterparts in tuning the thermal conductivity. Moreover, high $E/\kappa$ ratios could be achieved in medium-entropy ceramics, as shown in Figure 1.8 [55].

By broadening the concept of HEMs, the compositional space for these materials increases significantly, and the degree of freedom in tuning the properties, particularly multiple properties at the same time, is rendered.

## References

1 Cantor, B. (2007). Stable and metastable multicomponent alloys. *Ann. Chim. Sci. Mat.* 32: 245–256.

2 He, Q., Ding, Z., Ye, Y. et al. (2017). Design of high-entropy alloy: a perspective from nonideal mixing. *JOM* 69: 2092–2098.

3 Zhang, Y., Zuo, T., Tang, Z. et al. (2014). Microstructures and properties of high-entropy alloys. *Prog. Mater. Sci.* 61: 1–93.

4 Inoue, A., Zhang, T., and Masumoto, T. (1990). Production of amorphous cylinder and sheet of $La_{55}Al_{25}Ni_{20}$ alloy by a metallic mold casting method. *Mater. Trans., JIM* 31: 425–428.

5 Peker, A. and Johnson, W.L. (1993). A highly processable metallic glass: $Zr_{41.2}Ti_{13.8}Cu_{12.5}Ni_{10.0}Be_{22.5}$. *Appl. Phys. Lett.* 63: 2342–2344.

6 Greer, A.L. (1993). Confusion by design. *Nature* 366: 303–304.

7 Lin, X. and Johnson, W.L. (1995). Formation of Ti–Zr–Cu–Ni bulk metallic glasses. *Appl. Phys. Lett.* 78: 6514–6519.

8 Lin, X., Johnson, W.L., and Rhim, W.K. (1997). Effect of oxygen impurity on crystallization of an undercooled bulk glass forming Zr–Ti–Cu–Ni–Al alloy. *Mater. Trans., JIM* 38: 473–477.

9 Cantor, B., Kim, K.B., and Warren, P.J. (2002). Novel multicomponent amorphous alloys. *Mater. Sci. Forum* 386–388: 27–32.

10 Yeh, J., Chen, S., Lin, S. et al. (2004). Nanostructured high-entropy alloys with multiple principal elements: novel alloy design concepts and outcomes. *Adv. Eng. Mater.* 6: 299–303.

11 Cantor, B., Chang, I.T.H., Knight, P. et al. (2004). Microstructural development in equiatomic multicomponent alloys. *Mater. Sci. Eng., A* 375–377: 213–218.

12 Cantor, B. (2014). Multicomponent and high entropy alloys. *Entropy* 16: 4749–4768.

13 Gao, M.C., Yeh, J., Liaw, P.K. et al. (2016). *High-Entropy Alloys: Fundamentals and Applications*. Cham, Switzerland: Springer International Publishing.

14 Chen, T., Shun, T., Yeh, J. et al. (2004). Nanostructured nitride films of multi-element high-entropy alloys by reactive DC sputtering. *Surf. Coat. Technol.* 188, 189: 193–200.

15 Chen, T., Wong, M., Shun, T. et al. (2005). Nanostructured nitride films of multi-element high-entropy alloys by reactive DC sputtering. *Surf. Coat. Technol.* 200: 1361–1365.

16 Chen, T. and Wong, M. (2007). Structure and properties of reactively-sputtered $Al_xCoCrCuFeNi$ oxide films. *Thin Solid Films* 516: 141–146.

17 Rost, C.M., Sachet, E., Borman, T. et al. (2015). Entropy-stabilized oxides. *Nat. Commun.* 6: 8485.

18 Gild, J., Zhang, Y., Harrington, T. et al. (2016). High-entropy metal diborides: a new class of high-entropy materials and a new type of ultrahigh temperature ceramics. *Sci. Rep.* 6: 37946.

19 Yan, X.L., Constantin, L., Lu, Y.F. et al. (2018). $(Hf_{0.2}Zr_{0.2}Ta_{0.2}Nb_{0.2}Ti_{0.2})C$ high-entropy ceramics with low thermal conductivity. *J. Am. Ceram. Soc.* 101: 4486–4491.

20 Qin, Y., Liu, J., Li, F. et al. (2019). A high entropy silicide by reactive spark plasma sintering. *J. Adv. Ceram.* 8: 148–152.

21 Guan, J., Li, D., Yang, Z. et al. (2020). Synthesis and thermal stability of novel high-entropy metal boron carbonitride ceramic powders. *Ceram. Int.* 46: 26581–26589.

22 Yeh, J. (2013). Alloy design strategies and future trends in high-entropy alloys. *JOM* 65: 1759–1771.

**23** Zuo, T., Ren, S., Liaw, P.K. et al. (2013). Processing effects on the magnetic and mechanical properties of $FeCoNiAl_{0.2}Si_{0.2}$ high entropy alloy. *Int. J. Miner. Metall. Mater.* 20: 549–555.

**24** Yao, Y., Huang, Z., Hughes, L.A. et al. (2021). Extreme mixing in nanoscale transition metal alloys. *Matter* 4: 2340–2353.

**25** Liao, Y., Li, Y., Zhao, R. et al. (2022). High-entropy-alloy nanoparticles with 21 ultra-mixed elements for efficient photothermal conversion. *Nat. Sci. Rev.* nwac041. https://doi.org/10.1093/nsr/nwac041.

**26** Sarkar, A., Wang, Q., Schiele, A. et al. (2019). High-entropy oxides: fundamental aspects and electrochemical properties. *Adv. Mater.* 31: 1806236.

**27** Yeh, J. (2006). Recent progress in high-entropy alloys. *Ann. Chim. Sci. Mat.* 31: 633–648.

**28** Pickering, E.J., Muñoz-Moreno, R., Stone, H.J. et al. (2016). Precipitation in the equiatomic high-entropy alloy CrMnFeCoNi. *Scr. Mater.* 113: 106–109.

**29** Otto, F., Dlouhý, A., Pradeep, K.G. et al. (2016). Decomposition of the single-phase high-entropy alloy CrMnFeCoNi after prolonged anneals at intermediate temperatures. *Acta Mater.* 112: 40–52.

**30** Zhang, Y., Zhou, Y., Lin, J. et al. (2008). Solid-solution phase formation rules for multi-component alloys. *Adv. Eng. Mater.* 10: 534–538.

**31** Yeh, J., Chen, S., Gan, J. et al. (2004). Formation of simple crystal structures in Cu–Co–Ni–Cr–Al–Fe–Ti–V alloys with multiprincipal metallic elements. *Metall. Mater. Trans. A* 35A: 2533–2536.

**32** Yeh, J., Chang, S., Hong, Y. et al. (2007). Anomalous decrease in X-ray diffraction intensities of Cu–Ni–Al–Co–Cr–Fe–Si alloy systems with multi-principal elements. *Mater. Chem. Phys.* 103: 41–46.

**33** Owen, L.R., Pickering, E.J., Playford, H.Y. et al. (2017). An assessment of the lattice strain in the CrMnFeCoNi high-entropy alloy. *Acta Mater.* 122: 11–18.

**34** Jiang, B., Bridges, C.A., Unocic, R.R. et al. (2021). Probing the local site disorder and distortion in pyrochlore high-entropy oxides. *J. Am. Chem. Soc.* 143: 4193–4204.

**35** Oh, H., Duancheng, M., Leyson, G. et al. (2016). Lattice distortions in the FeCoNiCrMn high entropy alloy studied by theory and experiment. *Entropy* 18: 321.

**36** Rost, C.M., Rák, Z., Brenner, D.W. et al. (2017). Local structure of the $Mg_xNi_xCo_xCu_xZn_xO$ ($x = 0.2$) entropy-stabilized oxide: an EXAFS study. *J. Am. Ceram. Soc.* 100: 2732–2738.

**37** Zou, Y., Maiti, S., Steurer, W. et al. (2014). Size-dependent plasticity in an $Nb_{25}Mo_{25}Ta_{25}W_{25}$ refractory high-entropy alloy. *Acta Mater.* 65: 85–97.

**38** Jin, K., Sales, B.C., Stocks, G.M. et al. (2016). Tailoring the physical properties of Ni-based single-phase equiatomic alloys by modifying the chemical complexity. *Sci. Rep.* 6: 20159.

**39** Tsai, K., Tsai, M., and Yeh, J. (2013). Sluggish diffusion in Co–Cr–Fe–Mn–Ni high-entropy alloys. *Acta Mater.* 61: 4887–4897.

**40** Miracle, D.B. and Senkov, O.N. (2017). A critical review of high entropy alloys and related concepts. *Acta Mater.* 122: 448–511.

**41** Jin, K., Lu, C., Wang, L.M. et al. (2016). Effects of compositional complexity on the ion-irradiation induced swelling and hardening in Ni-containing equiatomic alloys. *Scr. Mater.* 119: 65–70.

**42** Zhao, Z., Xiang, H., Dai, F. et al. (2019). $(La_{0.2}Ce_{0.2}Nd_{0.2}Sm_{0.2}Eu_{0.2})_2Zr_2O_7$: a novel high-entropy ceramic with low thermal conductivity and sluggish grain growth rate. *J. Mater. Sci. Technol.* 35: 2647–2651.

**43** Ranganathan, S. (2003). Alloyed pleasures: multimetallic cocktails. *Curr. Sci.* 85: 1404–1406.

**44** Kao, Y., Chen, T., Chen, S. et al. (2009). Microstructure and mechanical property of as-cast, -homogenized, and -deformed $Al_xCoCrFeNi$ ($0 \le x \le 2$) high-entropy alloys. *J. Alloys Compd.* 488: 57–64.

**45** Zhang, Y., Zuo, T.T., Cheng, Y.Q. et al. (2013). High-entropy alloys with high saturation magnetization, electrical resistivity, and malleability. *Sci. Rep.* 3: 1455.

**46** Laplanche, G., Gadaud, P., Bärsch, C. et al. (2018). Elastic moduli and thermal expansion coefficients of medium-entropy subsystems of the CrMnFeCoNi high-entropy alloy. *J. Alloys Compd.* 746: 244–255.

**47** Zhao, Z., Chen, H., Xiang, H. et al. (2020). High-entropy $(Nd_{0.2}Sm_{0.2}Eu_{0.2}Y_{0.2}Yb_{0.2})_4Al_2O_9$ with good high temperature stability, low thermal conductivity and anisotropic thermal expansivity. *J. Adv. Ceram.* 9: 595–605.

**48** Ridley, M., Gaskins, J., Hopkins, P. et al. (2020). Tailoring thermal properties of multi-component rare earth monosilicates. *Acta Mater.* 195: 698–707.

**49** Li, Z., Pradeep, K.G., Deng, Y. et al. (2016). Metastable high-entropy dual-phase alloys overcome the strength-ductility trade-off. *Nature* 534: 227–230.

**50** Lu, Y., Dong, Y., Guo, S. et al. (2014). A promising new class of high-temperature alloys: eutectic high-entropy alloys. *Sci. Rep.* 4: 6200.

**51** Lu, Y., Jiang, H., Guo, S. et al. (2017). A new strategy to design eutectic high-entropy alloys using mixing enthalpy. *Intermetallics* 91: 124–128.

**52** Zhang, Y. (2019). *High-Entropy Materials: A Brief Introduction*. Singapore: Springer Nature Singapore Pvt Ltd.

**53** Wright, A.J., Wang, Q., Huang, C. et al. (2020). From high-entropy ceramics to compositionally-complex ceramics: a case study of fluorite oxides. *J. Eur. Ceram. Soc.* 40: 2120–2129.

**54** Wright, A.J., Wang, Q., Ko, S.-T. et al. (2020). Size disorder as a descriptor for predicting reduced thermal conductivity in medium- and high-entropy pyrochlores. *Scr. Mater.* 181: 76–81.

**55** Wright, A.J. and Luo, J. (2020). A step forward from high-entropy ceramics to compositionally complex ceramics: a new perspective. *J. Mater. Sci.* 55: 9812–9827.